

ADVANCED COHESIVE ZONE MODELS FOR FRACTURE SIMULATION

Thomas Siegmund

School of Mechanical Engineering, Purdue University,
West Lafayette, IN 47907-1288, U.S.A.

ABSTRACT

Cohesive zone models (CZM) are attractive for fracture process simulation since they provide a link between failure at the micro-scale and macro-scale structural response. Throughout the recent past many successful applications of CZMs have been reported. To further expand the scope of CZM, the development of improved constitutive equations for the description of the mechanical processes during material separation are needed. The present paper reports on several recent developments on CZM that incorporate aspects such as triaxiality, rate dependence, damage accumulation during cyclic loading, as well as coupling to heat transfer.

KEYWORDS

Finite element modeling, Cohesive zone, Ductile fracture, Adhesive, Fatigue crack, Heat transfer

INTRODUCTION

In the recent past it has become evident that the framework of classical fracture mechanics – despite its significant success – possesses a series of limitations as a predictive tool [1]. To obtain a more fundamental view of failure it is necessary to adopt a concept in which the competing actions of (1) material separation processes in the cohesive zone at and near the crack front, *i.e.* in the cohesive zone, and (2) the deformation of material elements surrounding the fracture process zone, determine the observed behavior of a structure. This type of failure analysis becomes possible if the stress strain behavior of a material as well as the *material separation behavior* is described by an appropriate constitutive equation.

In the cohesive zone model (CZM) approach, the material separation behavior is described in a constitutive equation relating the crack surface tractions, \mathbf{T}_{CZ} , to the displacement jump across the crack, $\mathbf{\Delta}$. This law represents the physical processes of material deterioration in the fracture process zone. Its material parameter are the cohesive strength, σ_{max} , the peak traction, the cohesive length, δ , the value of displacement jump across the crack at which the stress carrying capacity has fallen to zero, and the cohesive energy, ϕ , the area under the traction-separation curve. Within the

mechanical equilibrium statement written as the principle of virtual work the cohesive zone elements are accounted for as internal surfaces:

$$\int_V \mathbf{s} : \delta \mathbf{F} \, dV - \int_{S_{int}} \mathbf{T}_{CZ} \cdot \delta \mathbf{\Delta} \, dS = \int_{S_{ext}} \mathbf{T}_e \cdot \delta \mathbf{u} \, dS \quad (1)$$

Contributions in the volume and external surface terms (on V and S_{ext}) are described by the nominal stress tensor, $\mathbf{s} = \mathbf{F}^{-1} \det(\mathbf{F}) \boldsymbol{\sigma}$, with $\boldsymbol{\sigma}$ the Cauchy stress, the displacement vector, \mathbf{u} , the deformation gradient, \mathbf{F} , as well as by the traction vector, \mathbf{T}_e , on the external surface of the body. Traction vectors are related to \mathbf{s} by $\mathbf{T} = \mathbf{n} \mathbf{s}$, with \mathbf{n} being the surface normal. The cohesive surface contribution is described by the integral over the internal surface, S_{int} .

The concept of a cohesive fracture process zone abandons the failure criterion used in classical fracture mechanics and crack growth resistance of a structure is now viewed as the sum of the energy dissipated in the plastic zone and the energy spent in the actual separation process.

The basic concepts of CZM models are due to [2,3]. Current CZM models [4] differ from these classical models in that no initial crack needs to be defined and crack nucleation can thus be accounted for. Also, the length of the cohesive zone is not a parameter of the model. CZM models have been used in studies of monotonic or dynamic loading situations in homogeneous materials, composites and at interfaces. An overview paper [1] summarizes several examples of recent developments. Despite this success, few developments have been reported that aim at the development of improved traction separation laws. Such development can be accomplished if additional state variables are introduced into the CZM formulation [5]. The cohesive surface tractions are then no longer dependent on $\mathbf{\Delta}$ only. The present paper summarizes recent developments in this direction undertaken by the author. Approaches to computational modeling of ductile crack growth, rate dependency of failure, fatigue crack growth as well as fracture under thermo-mechanical loading are described.

TRIAXIALITY DEPENDENT CZM

Fracture of ductile materials is well known to be dependent on the level of constraint being present at the crack tip. Several prominent studies have clearly demonstrated that both the peak stress carrying capacity as well as the energy dissipated during void growth and coalescence can be characterized in terms of the stress triaxiality. While material models specifically geared towards failure based on void growth, *e.g.* the Gurson model [6], were specifically developed to account for the effect of triaxiality on material damage, CZMs have commonly assumed constant material parameter values for σ_{max} , δ or ϕ . This shortcoming can be overcome if these parameters are made dependent on the stress triaxiality. Since this quantity is not defined within the CZM itself, the effects of local crack tip constraint on the CZM parameters are introduced in dependence of the stress triaxiality in the solid elements adjacent to the crack line.

In a numerical study on ductile crack growth in a high strength structural steel, [7], the dependence of the CZM parameters on stress triaxiality was determined by unit cell simulations. The CZM parameters normalized by the flow strength of the material, σ_0 , and the void spacing, λ , respectively, are given in Fig. 1a in dependence of the maximum value of stress triaxiality reached during loading. Increasing triaxiality levels lead to an increase in σ_{max} and a decrease in ϕ . Subsequently, to study the effect of specimen size on the crack growth resistance a CZM with the CZM parameter dependence as of Fig. 1a was used. Both C(T) and M(T) specimens were analyzed. Figure 1b depicts the cohesive energy at $\Delta a = 20\lambda$ normalized by $(\sigma_0 \lambda)$ in dependence of the

normalized specimen size (W/X). The results clearly indicate that the cohesive energy, *i.e.* the energy needed to form new fracture surface, indeed is dependent on specimen size and geometry. The limit value of $\phi=0.5$ ($\sigma_{\max} X$) is reached only for fully developed crack tip constraint. Conventional CZMs cannot account for this effect.

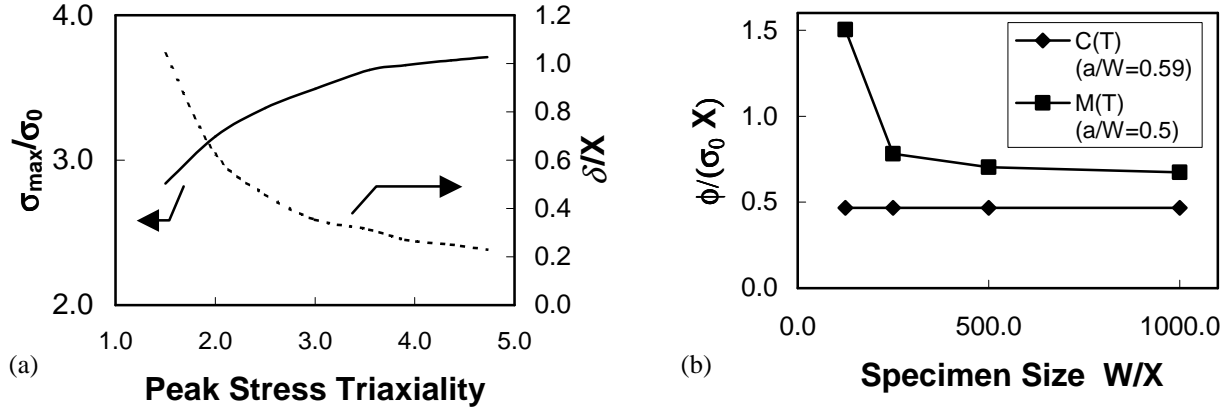


Figure 1: (a) Dependence of the normalized cohesive zone parameters on the peak value of stress triaxiality as obtained by unit cell computations of void growth, (b) Prediction of the normalized cohesive energy ($\Delta a=20 X$) in dependence of the normalized size for C(T) and M(T) specimens.

RATE DEPENDENT CZM FOR ADHESIVES

In studies of the integrity of adhesive bonds, CZM can conveniently be used to describe the combined deformation-failure behavior of the adhesive. To accurately describe polymeric adhesives it is necessary to account for the rate dependent fracture behavior exhibited by these materials.

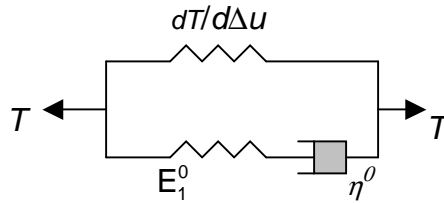


Figure 2: A rate-dependent CZM based on a standard linear solid model.

To capture such effects, a rate dependent CZM based on the standard linear solid was developed [8]. In this new CZM model (Figure 2), a rate-independent CZM, a secondary stiffness parameter, E_1^0 (force per displacement per area), and a viscosity, η^0 , (force per velocity per area) characterize the adhesive. To calibrate these parameters, fracture tests on DCB specimen bonded by a HDPE adhesives were performed for a wide range of applied loading speeds, V . A total of three tests were necessary to determine all CZM parameters. Figure 3a compares measured and predicted peak loads for DCB fracture tests. Subsequently, the new dependent CZM model was applied to investigate DCB tests with stepwise constant applied loading speeds. Figure 3b depicts the result of one of these tests. A good agreement between the experimental data and the numerical predictions was obtained. Especially, the short-term stress relaxation behavior was well captured.

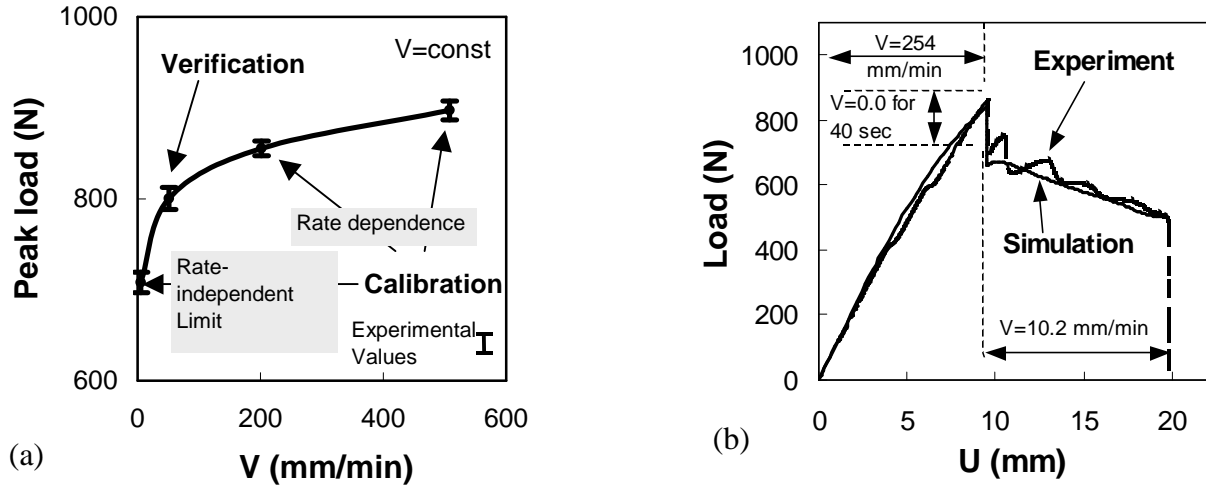


Figure 3: (a) Calibration of rate dependent CZM to peak loads of DCB tests at various crosshead speeds; (b) DCB test with three levels of crosshead speeds, simulation and experimental results.

CZM FOR FATIGUE CRACK GROWTH

For investigations of fatigue crack growth (FCG) the use of the Paris equation, $da/dN=A(\Delta G)^m$, to represent FCG data is a widely accepted approach [9]. However, this equation is empirical and provides a data correlation scheme rather than a predictive capability. This fact becomes especially important for interface FCG since experimentally determined $\Delta G-da/dN$ curves in this case depend on factors not of concern in homogeneous materials. Motivated by this need, it is attractive to extend CZMs to account for irreversible deformation, incorporate loading-unloading conditions and effects of accumulation of damage [10].

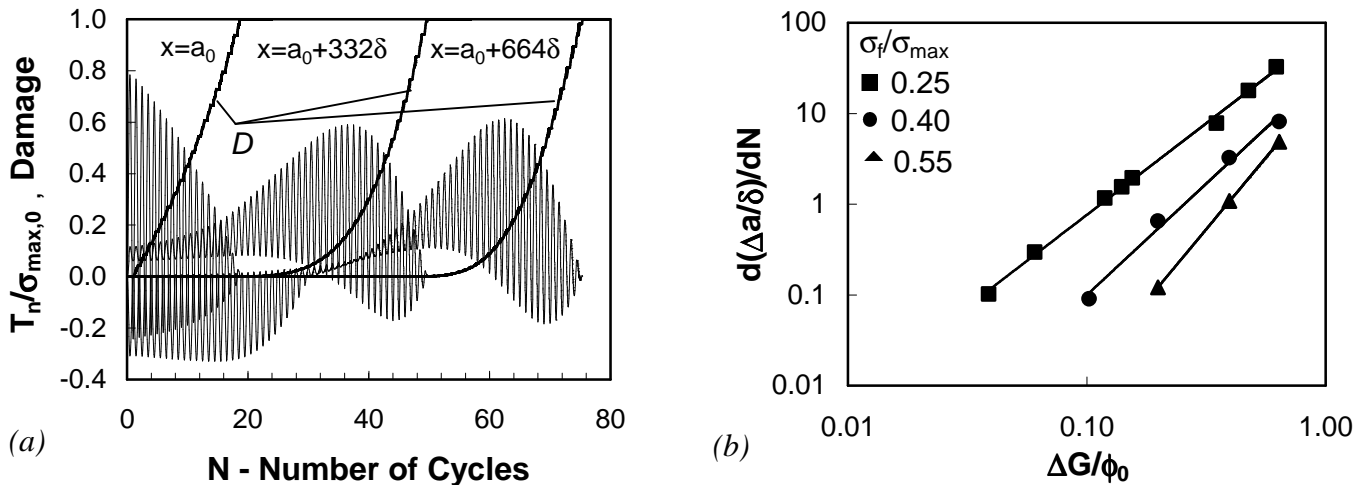


Figure 4: (a) The effective traction separation behavior accounting for unloading and damage dependent cohesive strength; (b) Numerically predicted fatigue crack growth rates for three values of the fatigue strength parameter, σ_f ; cyclic loading with $R=0$.

For cyclic loading, the evolution of the cohesive strength of the FPZ is accounted for by the use of a damage variable, D . The current cohesive strength is given as $\sigma_{\max} = \sigma_{\max,0} (1-D)$, where $\sigma_{\max,0}$ is the initial cohesive strength. For the case of mode I loading, the evolution of the damage variable, D , depends on the amount of the total accumulated displacement jump, Δ_{tot} , and on a fatigue limit stress, σ_f :

$$\dot{D} = \frac{|\dot{\Delta}_n|}{4\delta} \left[\frac{T_n}{\sigma_{\max}} - C \right] H(\Delta_{tot} - \delta) \quad \text{with} \quad \sigma_f = C \cdot \sigma_{\max}, \quad C < 1.0 \quad \Delta_{tot} = \int_t |\dot{\Delta}| dt \quad \text{if} \quad T_n > 0.0 \quad (2)$$

$$\dot{D} = 0 \quad \text{if} \quad T_n \leq 0$$

A parametric study of fatigue crack growth in an adhesively bonded DCB specimen was performed using a formulation accounting for Eqn. 2. Figure 4a depicts the evolution of both the crack surface traction and the damage variable as a function of the number of applied load cycles for three locations in the FPZ. Figure 4b summarizes the numerically obtained crack growth rates in dependence on the normalized applied $\Delta G/\phi_0$ for three levels of fatigue strength, σ_f . The numerically obtained $d(\Delta a/\delta)/dN$ values can be described by the use of the Paris relation. For the present choices of the fatigue limit ($C=0.25, 0.40, 0.55$) the predicted values of the Paris exponent, m , are 2.0, 2.5 and 3.1, respectively.

HEAT TRANSFER CZM

Past applications of the CZM were directed towards the analysis of mechanical loading only. In many situations, however, fracture is coupled to and influenced by other physical processes. As an example of interest, consider the thermal gradient loading of a composite with crack bridging fibers [11]; see Fig. 5 for a schematic drawing.

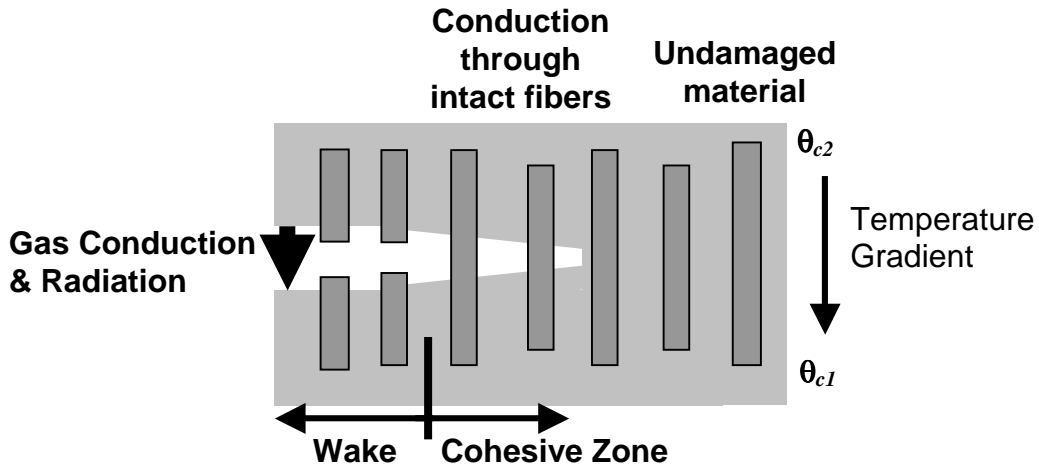


Figure 5: Thermo-mechanical processes during failure of a composite with bridging fibers.

A computational framework is required that allows for physically realistic fracture simulation for this thermo-mechanically coupled loading situations under the simultaneous consideration of crack growth and heat flux across the crack and the fracture process zone.

For a solution of this problem the system must fulfill thermodynamic equilibrium in addition to the mechanical equilibrium equation, Eqn. 1. In variational form and using Fourier's law, this can be expressed by:

$$\int_V \rho c_p (\partial_t \delta \theta) \delta \theta dV - \int_{S_{int}} h_{CZ} \Delta \theta \delta \Delta \theta dS + \int_V \frac{\partial \delta \theta}{\partial \mathbf{x}} \cdot \mathbf{k} \cdot \frac{\partial \delta \theta}{\partial \mathbf{x}} dV = \int_V \delta \theta r dV + \int_{S_{ext}} \delta \theta q dS \quad (3)$$

The volume and external surface contribution (on V and S_{ext}) are described by the temperature field, θ , the material density, ρ , the heat capacity, c_p , the conductivity matrix, \mathbf{k} , the heat flux per unit area of the body flowing into the body, q , and the heat supplied externally into the body per unit volume, r . The cohesive zone contributions, representing the crack wake and the process zone in front of the crack tip, are again described by the integral described by the integral over the internal surface, S_{int} . Two quantities describe the conductance across the cohesive zone: the cohesive zone conductance, h_{CZ} , and the temperature jump across the cohesive surface, $\Delta \theta = \theta_{C1} - \theta_{C2}$, with θ_{C1} and θ_{C2} the temperatures of the opposite crack surfaces. The coupling between stress and heat transfer part of the fracture problem as described by Eqns. (1) and (3), occurs via the cohesive zone conductance, h_{CZ} . This quantity, in general, is dependent not only on temperature but also on both the traction as well as the displacement jump, Δ , across the cohesive surface:

$$h_{CZ} = h_{CZ}(\theta, \mathbf{T}_{CZ}, \Delta) \quad (4)$$

The conductance law, Eqn. 4, describes the energy transport across cracks or delaminations. In the process zone h_{CZ} depends on the level of material deterioration and changes from that given by the solid to the crack wake conductance. In the crack wake, h_{CZ} is dominated by gas conductivity or radiation as well as possibly by the contact conductance of the two crack surfaces. Fully coupled thermo-mechanical analyses with repeated non-uniform and non-steady heat flow as well as secondary mechanical loads are possible with this approach. It describes the creation of new free surface and thus accounts for the changing heat transfer boundary conditions due to crack growth.

ACKNOWLEDGEMENT

Funding for the work was provided by Sandia National Laboratories through the NSF Life Cycle Engineering program as well as by Purdue University. The author would like to thank W. Brocks, GKSS Research Center Geesthacht, Germany, as well as C. Xu and K. Ramani, Purdue University, for their collaboration.

REFERENCES

1. Hutchinson, J.W. and Evans, A.G. (2000) *Acta Mat.* 48, 125.
2. Barenblatt, G.I. (1962) *Adv. Appl. Mech.* 7, 55.
3. Dugdale, D.S. (1960) *J. Mech. Phys Solids* 8, 100.
4. Needleman, A. (1987) *J. Appl. Mech.* 54, 525.
5. Needleman, A. (1992) *Ultramicroscopy* 40,203.
6. Gurson, A.L. (1977) *ASME J. Engng Mater. Tech.* 99, 2.
7. Siegmund, T. and Brocks, W. (2000) *Eng. Fract. Mech.* 67, 139.
8. Xu, C., Siegmund, T. and Ramani, K., (2001) *Int. J. Adhesives Adhesion*, submitted.
9. Paris, P.C., Gomez, M.P. and Anderson, W.P. (1961) *The Trend in Engng* 13, 9.
10. Roe, K.L. and Siegmund, T. (2001). In *1st MIT Conference on Computational Fluids and Solids Mechanics*, in print, Bathe, K.J. (Ed). Elsevier.
11. Hutchinson, J.W. and Lu, T.J. (1995) *ASME J. Eng. Mater.* 117, 386.